JACS
JOURNAL OF THE AMERICAN CHEMICAL SOCIETY
pubs.acs.org/JACS
Article

Targeted Protein Degradation through Fast Optogenetic Activation and Its Application to the Control of Cell Signaling

Amy Ryan, Jihe Liu, and Alexander Deiters*

Cite This: J. Am. Chem. Soc. 2021, 143, 9222–9229
Read Online

ABSTRACT: Development of methodologies for optically triggered protein degradation enables the study of dynamic protein functions, such as those involved in cell signaling, that are difficult to be probed with traditional genetic techniques. Here, we describe the design and implementation of a novel light-controlled peptide degron conferring N-end pathway degradation to its protein target. The degron comprises a photocaged N-terminal amino acid and a lysine-rich, 13-residue linker. By caging the N-terminal residue, we were able to optically control N-degron recognition by an E3 ligase, consequently controlling ubiquitination and proteasomal degradation of the target protein. We demonstrate broad applicability by applying this approach to a diverse set of target proteins, including EGFP, firefly luciferase, the kinase MEK1, and the phosphatase DUSP6 (also known as MKP3). The caged degron can be used with minimal protein engineering and provides virtually complete, light-triggered protein degradation on a second to minute time scale.

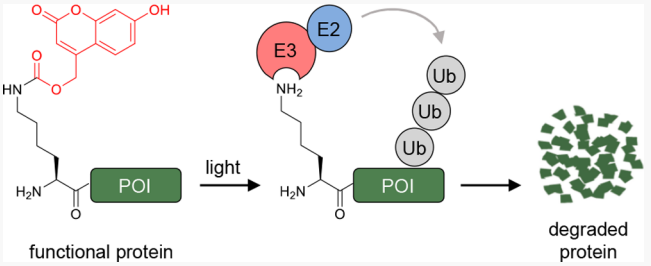

INTRODUCTION

Proteasomal degradation aids in maintaining cellular homeostasis through the turnover of misregulated, misfolded, or damaged proteins.[1] Several methodologies have harnessed this important cellular process to afford conditional control of protein activity, the most common of which include protein fusion to small molecule-controlled degradation domains (degrons) and small molecule inducers of degradation (PROTACs).[2−4] These approaches hold important advantages over small molecule inhibitors, namely, by retaining selectivity without being limited to the pool of "druggable" protein targets.[5]

The majority of small molecule-controlled degrons are based on engineered FRB and FKBP domains that are either stabilized or destabilized in the presence of suitable ligands such as rapamycin and related compounds.[6−11] Other approaches include the SMASh system, which utilizes a protease-degron fusion appended to the target protein and small molecule-mediated inhibition of the protease resulting in rapid destabilization and degradation.[12] HaloTag and IZFK3 degrons utilize hydrophobic/E3 ligand tagging[13,14] and E3 ligase recruitment,[15] respectively, for small molecule-induced degradation of protein fusions.

Optical systems for protein stability have been developed as well in order to achieve spatiotemporal control of cellular processes in a rapid, noninvasive manner while maintaining the above-mentioned advantages of degron protein engineering.[16] Examples include a photocaged small molecule dimerizer of the auxin-inducible domain (AID) and optogenetic approaches, such as LOV2-degron fusions for optical activation of protein degradation (B-LID)[17−19] and photoactivated cleavage of appended degron domain for optical deactivation of degradation (GLIMPSe).[20] Optical control over PROTAC function has been achieved through synthetic analogs bearing photoswitchable azobenzene linkers[21,22] and light-removable caging groups.[23−25]

While the technologies mentioned above offer optical control of target protein activity, these designs include certain limitations. The AID, B-LID, and GLIMPSe systems rely on large protein-fusions which risk interference with the endogenous function of the protein. LOV2-based technologies, including B-LID and GLIMPSe, are further limited by the need for long (hour time scale) irradiations, making time-resolved analysis of protein activity difficult. Light-regulated PROTAC technology lacks generalizability, as it requires prior knowledge of a selective and efficient PROTAC.

We developed a novel degron methodology employing a light-activated, short, 14-amino acid peptide for optical control of protein degradation through the N-end proteolytic pathway. This allows for rapid degradation of protein targets with minimal protein engineering and complete temporal control.

Received: April 26, 2021
Published: June 14, 2021

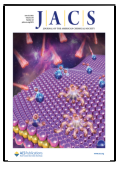

https://doi.org/10.1021/jacs.1c04324
J. Am. Chem. Soc. 2021, 143, 9222–9229

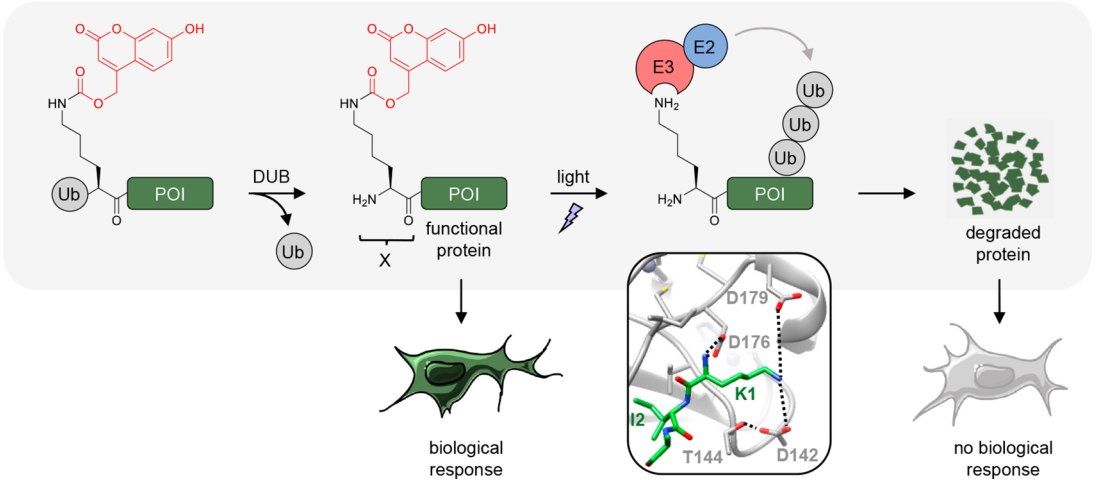

Figure 1. Light-inducible N-degron design. N-terminal ubiquitin is cotranslationally cleaved by endogenous DUBs, leaving a user-defined residue X, e.g., A, K, or the caged lysine, HCK. HCK-terminal proteins are stable until light exposure results in N-terminal decaging, E3 ligase recognition, E2 recruitment, polyubiquitination, and proteolytic degradation of the POI. Structure of the tetrapeptide KIAA (green) bound to the UBR box of UBR1 (gray). Dotted lines represent electrostatic interactions between the N-terminal lysine and negatively charged aspartic acid residues in UBR2. PDB: 3NII.

RESULTS AND DISCUSSION

Classically, the N-end pathway is defined as the process through which the half-life of a protein is determined by the N-terminal and, to a lesser extent, penultimate residues.[26] It is important in several regulatory and developmental processes.[27−31] A primary destabilizing residue, or N-degron, can be directly exposed in mammalian cells through the activity of endogenous proteases.[32] A general pathway for generation of destabilizing N-degrons (e.g., terminal lysine) is through proteolytic cleavage of pre-N-degrons by proteases such as endopeptidases, caspases, separase, and calpains.[33−35] While the resulting exposure of a stabilizing residue (e.g., alanine) does not alter protein half-life, exposure of a destabilizing residue (e.g., lysine) initiates the recruitment of proteasomal machinery.[36] The UBR class of E3 ligases recognizes N-degron motifs, and the crystal structure of an N-terminal lysine tetrapeptide bound to the UBR box of UBR1 reveals electrostatic interactions between the positively charged amino groups and the negatively charged binding pocket of the E3 ligase (Figure 1).[26] This is the only available cocrystal structure of a lysine terminal peptide docking to a UBR binding pocket. However, this process of targeted protein degradation can be achieved through the recognition of a lysine N-degron by four different mammalian proteins that encode the UBR box and recognize positively charged residues: UBR1, UBR2, UBR4, and UBR5.[37] UBR recruitment leads to the polyubiquitination of one or multiple internal lysines, labeling the protein for proteasomal degradation.[1]

In order to achieve optical control over this process, we hypothesized that by genetically introducing a photocaged hydroxycoumarin lysine (HCK)[38] at the N-terminal position, recognition by E3 ligases such as UBR1 will be blocked through steric bulk and disruption of the electrostatic interactions. Brief exposure to 365 or 405 nm light removes the caging group, restores the native degron, and leads to recruitment of either UBR1, UBR2, UBR4, or UBR5. To generate a methionine-free, N-terminal lysine, we designed a fusion containing an N-terminal ubiquitin that is cotranslationally cleaved by endogenous deubiquitinases.[39] Two control constructs were generated, exposing either alanine or lysine at the N-terminus of the protein of interest (POI): ADeg-POI and KDeg-POI, representing stabilized or destabilized proteins.[36] A light-controlled optoDeg was generated by replacing the N-terminal lysine with HCK, and is expected to remain stable and functional until the N-degron is exposed through photolysis, resulting in rapid proteasomal degradation of the POI.

We first sought to maximize instability of the degron, thus increasing the degradation efficiency of the POI. Previous studies have correlated the lysine density of an N-degron peptide with protein degradation, revealing that the strongest N-degrons contain 3 to 5 internal lysine residues.[40] In light of this, two unstructured linkers with randomized amino acid sequences and two different lengths (13- and 17-residues to accommodate up to 3 and 4 lysines, respectively) were modified with extra lysines at various distances from the primary residue (XDeg, Figure 2a). Mutation positions were chosen for their distance from the first four residues, which directly interact with the E3 ligase and determine UBR box recognition.[26,41] To accurately quantify degradation efficiency of the resulting fusion protein, we inserted a P2A self-cleavable linker between the N-degron-linked POI and a stable control protein.[42] The stability (and subsequent activity) of the POI is normalized to the stable internal control, reducing error from variable protein expression levels.

To quantitatively assess the degradation efficiency of the N-degron peptides, we first targeted an HA-tagged firefly luciferase,[43] using *Renilla* luciferase as the internal control (XDeg-FLuc-HA-P2A-RLuc). The FLuc degron variants were transiently expressed in HEK293T cells, and cells were exposed to light or kept in the dark. We utilized the dual luciferase assay to evaluate the extent of protein degradation. Assessment of KDeg-FLuc activity relative to the RLuc internal control revealed a trend in which increasing lysine content within the linker corresponded to increased instability, leading up to 85% degradation of constitutively active KDeg-FLuc constructs (Figure 2b, light green). Notably, increasing lysine density had no significant impact on optoDeg-FLuc stability after UV irradiation (Figure 2b, dark green). This may be due to a saturation of proteasomal machinery by the acutely

https://doi.org/10.1021/jacs.1c04324
J. Am. Chem. Soc. 2021, 143, 9222−9229

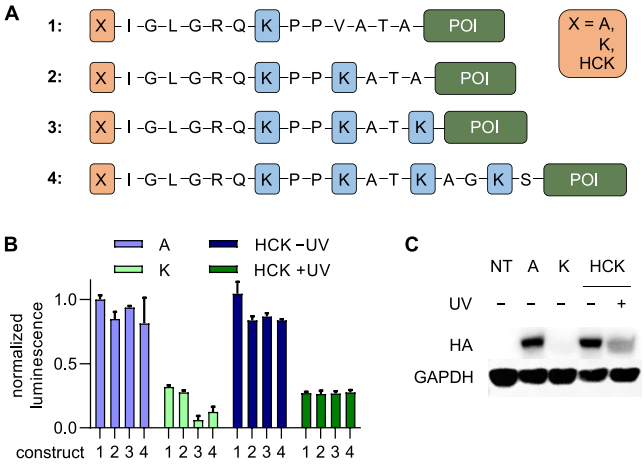

Figure 2. Light-activated degradation of firefly luciferase in HEK293T cells. (a) N-degron sequences with X representing the N-terminal A, K, or HCK. FLuc-HA was used as the protein of interest (POI) in the experiments shown here. (b) Comparison of the degradation efficiency of firefly luciferase (FLuc) in HEK293T cells. FLuc luminescence was normalized to RLuc as an internal control. OptoDeg-FLuc was kept in the dark (−UV) or irradiated with 365 nm light for 2 min (+UV). Error bars denote standard deviations from three biological replicates. (c) Validation of HA-tagged A, K, and HCK (±UV) stability through Western blot analysis of construct 3.

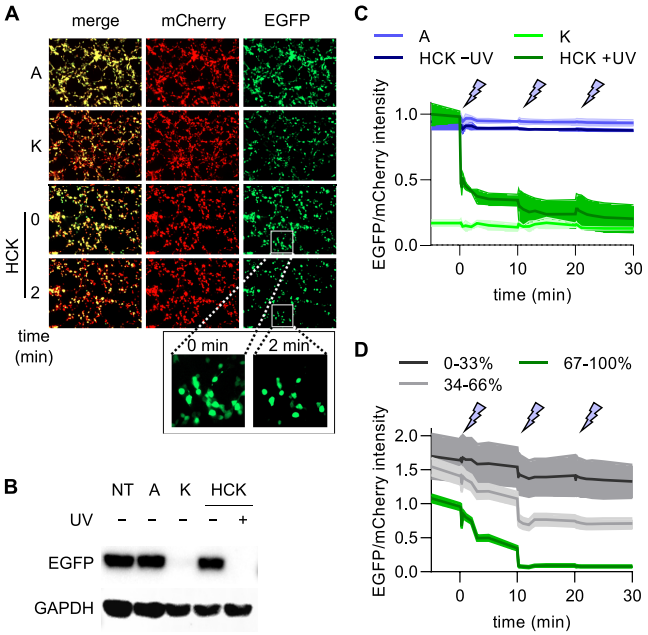

Figure 3. Light activated degradation of EGFP in HEK293T cells. (a) Stability of ADeg- and optoDeg-EGFP (−UV), and instability of KDeg- and optoDeg-EGFP (+UV), as verified through fluorescence microscopy. (b) Validation of A, K, and HCK (±UV) stability through Western blot analysis of EGFP expression. (c) Intensity of EGFP fluorescence relative to mCherry internal control at various time points pre- and postirradiation (labeled with blue lightning). $p < 0.0001$ from two-way ANOVA between HCK (+UV) and HCK (−UV) at $t = 30$ min. (d) Single cell analysis of EGFP fluorescence intensity relative to mCherry internal control at various time points pre- and postirradiation (labeled with blue lightning). Cells binned according to percent decrease of EGFP intensity relative to preirradiation intensity. A = ADeg-EGFP-P2A-mCherry; K = KDeg-EGFP-P2A-mCherry; HCK = optoDeg-EGFP-P2A-mCherry.

triggered degron, resulting in limitation of immediate optoDeg-FLuc degradation. While ADeg-FLuc stability was not affected by lysine doping, the same mutations resulted in decreased expression of optoDeg-FLuc relative to construct 1 (Figure 2b, light blue and dark blue, respectively). These results indicate that all constructs were suitable for efficient optically activated protein degradation; however, construct 3 was selected for further applications since it showed the lowest protein level for KDeg-Fluc. Western blot analysis of XDeg-FLuc stability in HEK293T cells revealed significantly lower levels of both KDeg- and optoDeg-FLuc (+UV) compared to those of ADeg- and optoDeg-FLuc (−UV) (Figure 2c). These results support the successful development of a small, light-activated degron that maintains protein levels matching those of stable protein controls prior to irradiation and triggers near-complete protein degradation upon light stimulation.

In order to assess both the robustness and the kinetics of the optically triggered N-degron, we applied the technology to different protein targets, including enhanced green fluorescent protein (EGFP). Using a P2A-linked mCherry internal control,[42] we assessed the caged degron using fluorescence microscopy (XDeg-EGFP-P2A-mCherry). The EGFP degron variants were transiently expressed in HEK293T cells, and the stability of the degron was monitored in the absence or presence of light. ADeg- and optoDeg-EGFP (−UV) controls displayed stable expression of EGFP (Figure 3a, first and third rows, respectively). Cells expressing KDeg-EGFP, in contrast, displayed reduced EGFP levels relative to the mCherry internal translation control (Figure 3a, second row). Degradation of optoDeg-EGFP was rapid upon light stimulation (405 nm, 60 s) and resulted in significant protein degradation within minutes of irradiation (Figure 3a, bottom row). However, degradation was incomplete, as evident from residual EGFP fluorescence in irradiated cells. As previously discussed, we attribute this to oversaturation of the proteasomal machinery in response to high levels of destabilized protein. To address this, protein expression was inhibited through either incubation with the translational inhibitor cycloheximide[44] (in case of experiments with ADeg and KDeg) or simple withdrawal of the unnatural amino acid HCK (in case of optoDeg) upon treatment with light, followed by a 24 h incubation period for proteasomal degradation of the destabilized constructs. Western blot analysis revealed protein stability of ADeg- and optoDeg-EGFP (−UV) and complete degradation of KDeg- and optoDeg-EGFP (+UV) (365 nm, 2 min) following translational inhibition (Figure 3b). Complete degradation of optoDeg-EGFP can likely be attributed to the long (24 h) incubation period for proteasomal processing of the saturated protein postirradiation.

While fluorescence microscopy analysis showed rapid and extensive protein degradation, the results did not match the high level of degradation observed using Western blot analysis. We hypothesized that an acute increase of decaged protein can overwhelm the proteasomal machinery; we therefore analyzed degron stability on a single-cell basis over time in order to investigate the relationship between protein expression level and extent of degradation. ADeg-, KDeg-, and optoDeg-EGFP were transiently expressed in HEK293T cells and treated with or without light in three consecutive exposures followed by 10 min incubation periods, during which cells were monitored using fluorescence microscopy. Resulting EGFP/mCherry values were subsequently evaluated on a single cell level both for the entire population ($n = 100$) and binned according to

https://doi.org/10.1021/jacs.1c04324
J. Am. Chem. Soc. 2021, 143, 9222−9229

the level of protein degradation. While population-level expression of ADeg- and KDeg-EGFP negative and positive controls were not significantly altered upon irradiation, light-induced decaging of optoDeg-EGFP resulted in degron activation and considerable degradation of the destabilized protein, closely resembling KDeg-EGFP levels (Figure 3c). We utilized light titration to visualize the rapid decrease in protein expression, especially within the first ten seconds of protein decaging. Relative EGFP fluorescence was monitored over the course of 10 min after each 15 s irradiation. OptoDeg-EGFP degradation was extremely rapid upon initial irradiation, reaching 50% degradation within the first minute and increasing to 80% degradation as additional irradiation further increased decaging and thus increased protein instability, demonstrating tunability of protein levels through a simple adjustment of light exposure.

In order to better understand the relationship between initial cellular EGFP concentration and the level of protein degradation, cells were binned and grouped by the percentage of EGFP loss relative to the initial (−UV) time point (Figure 3d). Cells displaying 0 to 33% EGFP degradation (n = 8) have an average EGFP/mCherry fluorescence ratio of about 1.64 at the 0 min time point and show a rather gradual decrease in EGFP expression over time. Cells reaching 34−66% EGFP degradation (n = 16) and 67−100% EGFP degradation (n = 76; the majority of cells) display a lower average EGFP/mCherry fluorescence of about 1.41 and 0.959, respectively. Loss of fluorescence in cells expressing lower initial EGFP fluorescence was rapid, reaching near complete degradation immediately upon the second irradiation at 10 min. These results revealed an inverse correlation between initial POI levels and degradation efficiency, presumably due to over-saturation of the proteasomal machinery.[45−47] This correlation is consistent with the increased level of protein degradation observed in translationally inhibited cells after 24 h, compared to a shorter (30 min) degradation period. POI levels suitable for rapid degradation via optoDeg should be readily achievable through simple concentration adjustments of HCK, which directly impacts protein expression levels.[48]

Cell signaling processes are rapid and highly dynamic and thus benefit from optical control and perturbation approaches.[49,50] We selected MKP3, a dual-specificity phosphatase with regulatory functions in cellular processes such as proliferation, differentiation, and development, as a target for our optoDeg methodology. MKP3 is transcriptionally activated in response to ERK/MAPK signaling and is responsible for negative feedback regulation of ERK though the direct dephosphorylation and deactivation of its cytoplasmic population.[51] This prevents the nuclear translocation and subsequent kinase activity of ERK, inhibiting activation of transcriptional programs. This feedback attenuation serves to dampen MAPK signaling at the ERK node, and previous studies have linked this process to the regulation of axial patterning in development.[52] The catalytically dead C293S mutant of MKP3 (dMKP3) presents a dominant negative mutant in which the inactive enzyme retains affinity for pERK without the ability to catalyze its dephosphorylation. This results in pERK sequestration by the phosphatase in the cytoplasm, restricting pERK's interaction not only with other catalytically active proteins but also with nuclear substrates (Figure 4a).[53,54] By fusing our optically controlled N-degron to dMKP3, we hypothesized that ERK translocation would be blocked until light exposure. In order to test this, we utilized an

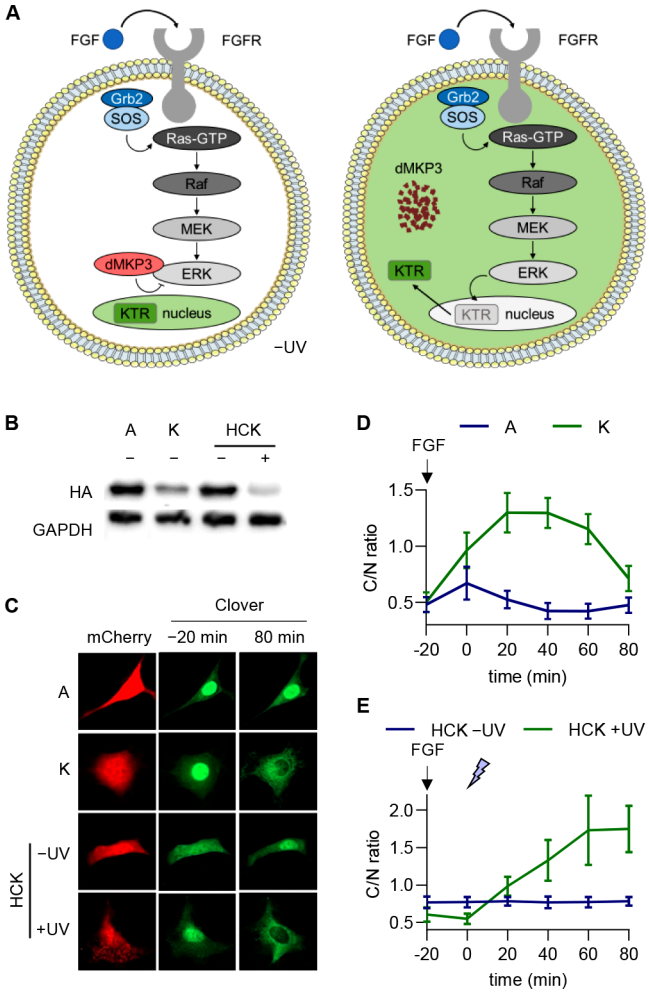

Figure 4. Control of ERK signaling through light activated degradation of dMKP3 in NIH 3T3 cells. (a) Schematic of the ERK/MAPK signaling pathway. (b) Validation of HA-tagged A, K, and HCK (±UV) stability through Western blot analysis. (c) Representative fluorescence microscopy images of NIH 3T3 cells expressing A, K, and HCK (±UV). (d) Time-course quantification of C/N ratio of Clover fluorescence pre- and poststimulation in cells expressing A or K. (e) Time-course quantification of C/N ratio of Clover fluorescence pre- and postirradiation in stimulated cells expressing HCK (−UV) or HCK (+UV). p = 0.0003 from two-way ANOVA for HCK (+UV) at t = 0 min and t = 80 min. Error bars represent standard error of the mean from 10 to 12 individual cells combined from three biological replicates. A = ADeg-dMKP3-P2A-mCherry; K = KDeg-dMKP3-P2A-mCherry; HCK = optoDeg-dMKP3-P2A-mCherry.

ERK KTR-Clover reporter that contains four main components: (1) the kinase binding domain of an ERK substrate (Elk1), (2) a nuclear localization sequence (deactivated through phosphorylation), (3) a nuclear export sequence (activated through phosphorylation), and (4) a Clover green fluorescent protein.[55]

We again used the P2A linker for validation of dMKP3 translation and HCK incorporation through mCherry fluorescent protein expression (XDeg-dMKP3-HA-P2A-mCherry). The dMKP3 degron variants were transiently expressed in HEK293T cells. The cells were simultaneously treated with light (365 nm, 2 min) and transcriptionally inhibited through either HCK withdrawal (optoDeg-dMKP3) or cycloheximide treatment (ADeg- and KDeg-dMKP3). After another 24 h

https://doi.org/10.1021/jacs.1c04324
J. Am. Chem. Soc. 2021, 143, 9222−9229

incubation, Western blot analysis revealed stable expression of ADeg- and optoDeg-dMKP3 (−UV) compared to the extensive degradation of destabilized KDeg- and optoDeg-dMKP3 (+UV) (Figure 4b).

An ERK KTR-Clover reporter was used for the analysis of ERK activity in live cells in the presence of stabilized or destabilized dMKP3. NIH3T3 cells coexpressing the dMKP3 degron variants and the pERK-KTR-Clover reporter were serum starved for 6 h to minimize extracellular stimulation of ERK signaling. In the absence of MAPK signaling, the ERK KTR-Clover reporter was localized in the nucleus (t = −20 min). Upon FGF-induced activation of the ERK/MAPK pathway (t = −20 min), ERK phosphorylation of the reporter stimulated rapid nuclear exportation (t = 80 min) (Supporting Figure S1). Complete cytoplasmic accumulation of the KTR reporter was achieved within 20 min of stimulation in the absence of dMKP3. ERK sequestration was demonstrated through the maintenance of nuclear ERK KTR-Clover in cells expressing optoDeg-dMKP3 (−UV) (Figure 4c, third row; Figure 4e, blue). Irradiation of optoDeg-dMKP3 (405 nm, 60 s) following ERK/MAPK stimulation allows for complete proteolytic degradation within 20 min and resulted in release of pERK from the cytoplasm and activation of ERK KTR-Clover reporter upon cellular stimulation (Figure 4c, last row; Figure 4e, green). Nuclear exportation of the reporter plateaued about 20 min poststimulation. These results match the reporter response to FGF stimulation in the presence of the ADeg- and KDeg-dMKP3 controls (Figure 4c, first and second rows; Figure 4d, blue and green, respectively). Unexpectedly, some nuclear re-entry was observed in cells expressing KDeg-dMKP3. This is likely due to the compensatory effects of a low remaining KDeg-dMKP3 concentration, ERK suppression by phosphatases,[56] or a combination of the two. Ultimately, our results support the utility of the degron-fused dMKP3 variant for activation of ERK signaling in the presence of light.

After demonstrating optical deactivation of phosphatase function with our light-triggered degron, we turned to the regulation of kinase activity next. MEK1 is a protein kinase that is central to the Ras/MAPK cell signaling cascade through the phosphorylation and activation of ERK.[57] MEK1 activation is dependent on the phosphorylation of two key residues, Ser218 and Ser222, and introduction of aspartic acid mutations at these two sites generates a constitutively active enzyme (Figure 5a).[58] To evaluate the efficacy of the caged degron with caMEK1, we generated a construct bearing the P2A-mCherry internal control (XDeg-caMEK1-P2A-mCherry). Following expression of caMEK1 degron variants in HEK293T cells, we treated them with light (365 nm, 2 min) and translationally inhibited them through cycloheximide treatment (ADeg- and KDeg-caMEK1) or UAA removal (optoDeg-caMEK1). After overnight incubation ensured optimal protein degradation, Western blot analysis showed high protein levels for ADeg- and optoDeg-caMEK1 (−UV) and complete degradation of the destabilized KDeg- and optoDeg-caMEK1 (+UV) (Figure 5b), validating the efficiency of the caged degron with caMEK1.

The activity of the degron-fused caMEK1 was then analyzed using a fluorescently labeled ERK translocation reporter (EGFP-ERK2) in order to generate measurements using its direct downstream target. We analyzed the response of serum starved cells expressing EGFP-ERK2 to FGF-mediated stimulation to establish a baseline for EGFP-ERK2 activation

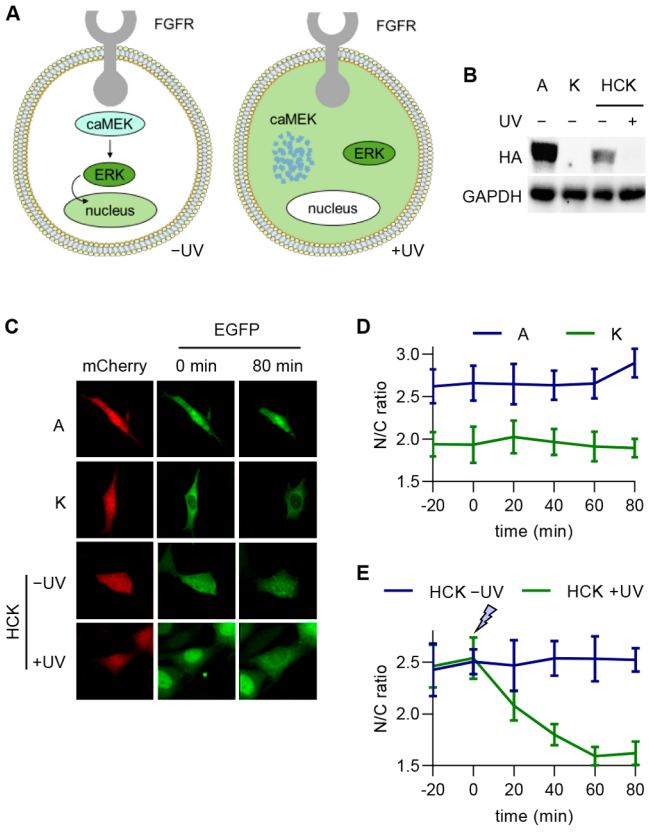

Figure 5. Control of ERK signaling through light activated degradation of caMEK1 in NIH 3T3 cells. (a) Schematic of the EGFP-ERK2 reporter mechanism. (b) Validation of HA-tagged A, K, and HCK (±UV) stability through Western blot analysis. (c) Representative fluorescence microscopy images of NIH 3T3 cells expressing ADeg-, KDeg-, or optoDeg-caMEK1. (d) Time-course quantification of N/C ratio of EGFP fluorescence over the course of 100 min in cells expressing A or K without external stimulation. (e) Time-course quantification of N/C ratio of EGFP fluorescence before (−20 to 0 min) and after (20 to 80 min) irradiation of cells expressing HCK compared to nonirradiated cells expressing HCK. p = 0.0054 from two-way ANOVA for HCK (+UV) at t = 0 min and t = 80 min. Error bars represent standard error of the mean from ten individual cells combined from three biological replicates. A = ADeg-caMEK1-P2A-mCherry; K = KDeg-caMEK1-P2A-mCherry; HCK = optoDeg-caMEK1-P2A-mCherry.

by endogenous signaling (t = 0 min) (SI Figure S2). This resulted in the phosphorylation and subsequent translocation of the reporter to the nucleus upon stimulation, with nuclear accumulation slowing after about 40 min. The nuclear/cytoplasmic ratio of the reporter in serum-starved cells expressing optoDeg-caMEK1 (−UV) displayed stable activation and nuclear accumulation of the EGFP-ERK2 reporter (Figure 5c, third row; Figure 5e, blue). These results match literature reports for MEK-induced translocation of the EGFP-ERK2 reporter in the same cell line.[59] Upon light-induced degradation of optoDeg-caMEK1, constitutive phosphorylation of the EGFP-ERK2 reporter was halted and cytoplasmic localization was restored after about 60 min (Figure 5c, last row; Figure 5e, green). Activity of the reporter in the presence of the stabilized or destabilized optoDeg-caMEK1 closely resembled the response observed with the ADeg-caMEK1 and KDeg-caMEK1 controls, respectively (Figure 5c, first and second rows; Figure 5d, blue and green, respectively).

https://doi.org/10.1021/jacs.1c04324
J. Am. Chem. Soc. 2021, 143, 9222−9229

Localization of the reporter was not significantly changed with irradiation over the course of 80 min in either of these controls, indicating that the light exposure itself had no effect on Ras/MAPK signaling. These results indicate that ERK activation is selectively turned off through the light-induced degradation of its upstream activator, MEK.

CONCLUSION AND SUMMARY

In conclusion, we developed a very small, light-inducible degron, optoDeg, for fast optical activation of protein degradation. Our design takes advantage of the N-end proteolytic pathway and includes a photocaged N-terminal lysine, directly appended to the protein of interest via a short, 13-amino acid peptide. The photocaged lysine was strategically placed in the N-terminal position to sterically restrict lysine binding to the recognition domain of UBR-type E3 ligases, thereby enabling acute optical control of the first step of the N-end pathway. Irradiation with 405 nm light induced the decaging of the terminal amino acid, leading to E3 ligase recruitment and subsequent target protein degradation by the proteasomal machinery. The extent of degradation was validated with both optoDeg-EGFP and optoDeg-FLuc constructs, reaching up to 85% degradation within minutes of irradiation. Complete, or near-complete, protein degradation after light stimulation was also confirmed by Western blots. The degradation kinetics were determined using the optoDeg-EGFP construct, revealing 65% degradation within 3 min of an initial 15 s irradiation and plateauing at 85% degradation within 3 min of a second light exposure. Thus, degradation can not only be rapidly induced (within seconds) but can be tuned depending on the level of light exposure. Further analysis of the fluorescence decrease in cells expressing optoDeg-EGFP on a single-cell basis through imaging cytometry after optical stimulation indicated a correlation between initial EGFP expression levels and the extent of degradation. Cells displaying only up to 33% decrease in EGFP fluorescence upon decaging express on average 70% more EGFP prior to irradiation than cells reaching near complete degradation of optoDeg-EGFP. This supports the hypothesis that increased protein expression can overwhelm N-end pathway machinery, ultimately decreasing proteolytic efficiency after acute activation.[45−47]

The versatility of the optoDeg approach was demonstrated through the light-induced, temporally controlled degradation of essential proteins in controlling the ERK/MAPK cell signaling pathway, including both the phosphatase dMKP3 and the kinase caMEK1. An optoDeg-dMKP3 construct was utilized to demonstrate acute temporal control of ERK signaling through the release of cytoplasmic sequestered pERK upon irradiation and degradation of dMKP3. Complete cellular response was observed within 20 min of stimulation in cells expressing the decaged optoDeg-dMKP3. Alternatively, optoDeg-caMEK1 was utilized for on-to-off control of ERK signaling upon light-triggered degradation of caMEK1.

The efficiency, flexibility, and complete specificity afforded by optoDeg are characteristics that, in combination, cannot be achieved with traditional genetic techniques, such that fast and virtually complete protein knockdown is obtained with precise external, light-triggered regulation and with limited protein engineering, adding only a very small peptide tag to the protein of interest. We expect our optically activated degron to aid in dissecting the complicated networks of cell signaling thus contributing to the growing pool of knowledge concerning important molecular mechanisms which govern cellular processes such as development and proliferation in both normal and disease-state models. Given the recent advances in genetic code expansion in animals, we expect this system to be also functional in worm, fly, fish, and mouse models.[60]

ASSOCIATED CONTENT

Supporting Information

This material is available free of charge at the ACS Web site. The Supporting Information is available free of charge at https://pubs.acs.org/doi/10.1021/jacs.1c04324.

Detailed biological protocols, additional micrographs and time-course data for ERK reporter controls, as well as primer sequences and plasmid maps (PDF)

AUTHOR INFORMATION

Corresponding Author

Alexander Deiters − *Department of Chemistry, University of Pittsburgh, Pittsburgh, Pennsylvania 15260, United States;* orcid.org/0000-0003-0234-9209; Email: deiters@pitt.edu

Authors

Amy Ryan − *Department of Chemistry, University of Pittsburgh, Pittsburgh, Pennsylvania 15260, United States*

Jihe Liu − *Department of Chemistry, University of Pittsburgh, Pittsburgh, Pennsylvania 15260, United States*

Complete contact information is available at: https://pubs.acs.org/10.1021/jacs.1c04324

Notes

The authors declare no competing financial interest.

ACKNOWLEDGMENTS

This work was supported by the National Science Foundation (CHE-1904972). We would like to thank Dr. Jason Haugh for kindly providing the pEGFP-ERK2 plasmid. We thank Dr. Markus Covert and Dr. Randall Moon for depositing Addgene plasmid nos. 59138 and 12456, respectively. We acknowledge lab member Chasity Hankinson for the synthesis of HCK.

REFERENCES

(1) Ciechanover, A.; Stanhill, A. The Complexity of Recognition of Ubiquitinated Substrates by the 26S Proteasome. *Biochim. Biophys. Acta, Mol. Cell Res.* **2014**, *1843* (1), 86−96.

(2) Paiva, S.-L.; Crews, C. M. Targeted Protein Degradation: Elements of PROTAC Design. *Curr. Opin. Chem. Biol.* **2019**, *50*, 111−119.

(3) Gao, H.; Sun, X.; Rao, Y. PROTAC Technology: Opportunities and Challenges. *ACS Med. Chem. Lett.* **2020**, *11* (3), 237−240.

(4) Coleman, K. G.; Crews, C. M. Proteolysis-Targeting Chimeras: Harnessing the Ubiquitin-Proteasome System to Induce Degradation of Specific Target Proteins. *Annu. Rev. Cancer Biol.* **2018**, *2* (1), 41−58.

(5) Ottis, P.; Crews, C. M. Proteolysis-Targeting Chimeras: Induced Protein Degradation as a Therapeutic Strategy. *ACS Chem. Biol.* **2017**, *12* (4), 892−898.

(6) Banaszynski, L. A.; Chen, L.; Maynard-Smith, L. A.; Ooi, A. G. L.; Wandless, T. J. A Rapid, Reversible, and Tunable Method to Regulate Protein Function in Living Cells Using Synthetic Small Molecules. *Cell* **2006**, *126* (5), 995−1004.

(7) Pratt, M. R.; Schwartz, E. C.; Muir, T. W. Small-Molecule-Mediated Rescue of Protein Function by an Inducible Proteolytic Shunt. *Proc. Natl. Acad. Sci. U. S. A.* **2007**, *104* (27), 11209−11214.

(8) Miyazaki, Y.; Imoto, H.; Chen, L.; Wandless, T. J. Destabilizing Domains Derived from the Human Estrogen Receptor. *J. Am. Chem. Soc.* **2012**, *134* (9), 3942−3945.
(9) Navarro, R.; Chen, L.; Rakhit, R.; Wandless, T. J. A Novel Destabilizing Domain Based on a Small-Molecule Dependent Fluorophore. *ACS Chem. Biol.* **2016**, *11* (8), 2101−2104.
(10) Pan, D.; Xuan, B.; Sun, Y.; Huang, S.; Xie, M.; Bai, Y.; Xu, W.; Qian, Z. An Intein-Mediated Modulation of Protein Stability System and Its Application to Study Human Cytomegalovirus Essential Gene Function. *Sci. Rep.* **2016**, *6* (1), 26167.
(11) Nabet, B.; Roberts, J. M.; Buckley, D. L.; Paulk, J.; Dastjerdi, S.; Yang, A.; Leggett, A. L.; Erb, M. A.; Lawlor, M. A.; Souza, A.; Scott, T. G.; Vittori, S.; Perry, J. A.; Qi, J.; Winter, G. E.; Wong, K.-K.; Gray, N. S.; Bradner, J. E. The DTAG System for Immediate and Target-Specific Protein Degradation. *Nat. Chem. Biol.* **2018**, *14* (5), 431−441.
(12) Hannah, J.; Zhou, P. A Small-Molecule SMASh Hit. *Nat. Chem. Biol.* **2015**, *11* (9), 637−638.
(13) Raina, K.; Noblin, D. J.; Serebrenik, Y. V.; Adams, A.; Zhao, C.; Crews, C. M. Targeted Protein Destabilization Reveals an Estrogen-Mediated ER Stress Response. *Nat. Chem. Biol.* **2014**, *10* (11), 957−962.
(14) Buckley, D. L.; Raina, K.; Darricarrere, N.; Hines, J.; Gustafson, J. L.; Smith, I. E.; Miah, A. H.; Harling, J. D.; Crews, C. M. HaloPROTACS: Use of Small Molecule PROTACs to Induce Degradation of HaloTag Fusion Proteins. *ACS Chem. Biol.* **2015**, *10* (8), 1831−1837.
(15) Koduri, V.; McBrayer, S. K.; Liberzon, E.; Wang, A. C.; Briggs, K. J.; Cho, H.; Kaelin, W. G. Peptidic Degron for IMiD-Induced Degradation of Heterologous Proteins. *Proc. Natl. Acad. Sci. U. S. A.* **2019**, *116* (7), 2539−2544.
(16) Courtney, T.; Deiters, A. Recent Advances in the Optical Control of Protein Function through Genetic Code Expansion. *Curr. Opin. Chem. Biol.* **2018**, *46*, 99−107.
(17) Delacour, Q.; Li, C.; Plamont, M.-A.; Billon-Denis, E.; Aujard, I.; Le Saux, T.; Jullien, L.; Gautier, A. Light-Activated Proteolysis for the Spatiotemporal Control of Proteins. *ACS Chem. Biol.* **2015**, *10* (7), 1643−1647.
(18) Renicke, C.; Schuster, D.; Usherenko, S.; Essen, L.-O.; Taxis, C. A LOV2 Domain-Based Optogenetic Tool to Control Protein Degradation and Cellular Function. *Chem. Biol.* **2013**, *20* (4), 619−626.
(19) Bonger, K. M.; Rakhit, R.; Payumo, A. Y.; Chen, J. K.; Wandless, T. J. General Method for Regulating Protein Stability with Light. *ACS Chem. Biol.* **2014**, *9* (1), 111−115.
(20) Mondal, P.; Krishnamurthy, V. V.; Sharum, S. R.; Haack, N.; Zhou, H.; Cheng, J.; Yang, J.; Zhang, K. Repurposing Protein Degradation for Optogenetic Modulation of Protein Activities. *ACS Synth. Biol.* **2019**, *8* (11), 2585−2592.
(21) Reynders, M.; Matsuura, B. S.; Bérouti, M.; Simoneschi, D.; Marzio, A.; Pagano, M.; Trauner, D. PHOTACs Enable Optical Control of Protein Degradation. *Sci. Adv.* **2020**, *6* (8), No. eaay5064.
(22) Pfaff, P.; Samarasinghe, K. T. G.; Crews, C. M.; Carreira, E. M. Reversible Spatiotemporal Control of Induced Protein Degradation by Bistable PhotoPROTACs. *ACS Cent. Sci.* **2019**, *5* (10), 1682−1690.
(23) Naro, Y.; Darrah, K.; Deiters, A. Optical Control of Small Molecule-Induced Protein Degradation. *J. Am. Chem. Soc.* **2020**, *142* (5), 2193−2197.
(24) Xue, G.; Wang, K.; Zhou, D.; Zhong, H.; Pan, Z. Light-Induced Protein Degradation with Photocaged PROTACs. *J. Am. Chem. Soc.* **2019**, *141* (46), 18370−18374.
(25) Kounde, C. S.; Shchepinova, M. M.; Saunders, C. N.; Muelbaier, M.; Rackham, M. D.; Harling, J. D.; Tate, E. W. A Caged E3 Ligase Ligand for PROTAC-Mediated Protein Degradation with Light. *Chem. Commun.* **2020**, *56* (41), 5532−5535.
(26) Matta-Camacho, E.; Kozlov, G.; Li, F. F.; Gehring, K. Structural Basis of Substrate Recognition and Specificity in the N-End Rule Pathway. *Nat. Struct. Mol. Biol.* **2010**, *17* (10), 1182−1187.
(27) Bachmair, A.; Finley, D.; Varshavsky, A. In Vivo Half-Life of a Protein Is a Function of Its Amino-Terminal Residue. *Science* **1986**, *234* (4773), 179−186.
(28) Zenker, M.; Mayerle, J.; Lerch, M. M.; Tagariello, A.; Zerres, K.; Durie, P. R.; Beier, M.; Hülskamp, G.; Guzman, C.; Rehder, H.; Beemer, F. A.; Hamel, B.; Vanlieferinghen, P.; Gershoni-Baruch, R.; Vieira, M. W.; Dumic, M.; Auslender, R.; Gil-Da-Silva-Lopes, V. L.; Steinlicht, S.; Rauh, M.; Shalev, S. A.; Thiel, C.; Winterpacht, A.; Kwon, Y. T.; Varshavsky, A.; Reis, A. Deficiency of UBR1, a Ubiquitin Ligase of the N-End Rule Pathway, Causes Pancreatic Dysfunction, Malformations and Mental Retardation (Johanson-Blizzard Syndrome). *Nat. Genet.* **2005**, *37* (12), 1345−1350.
(29) Brower, C. S.; Varshavsky, A. Ablation of Arginylation in the Mouse N-End Rule Pathway: Loss of Fat, Higher Metabolic Rate, Damaged Spermatogenesis, and Neurological Perturbations. *PLoS One* **2009**, *4* (11), No. e7757.
(30) Kwon, Y. T.; Kashina, A. S.; Davydov, I. V.; Hu, R.-G.; An, J. Y.; Seo, J. W.; Du, F.; Varshavsky, A. An Essential Role of N-Terminal Arginylation in Cardiovascular Development. *Science* **2002**, *297* (5578), 96−99.
(31) Hu, R.-G.; Wang, H.; Xia, Z.; Varshavsky, A. The N-End Rule Pathway Is a Sensor of Heme. *Proc. Natl. Acad. Sci. U. S. A.* **2008**, *105* (1), 76−81.
(32) Dougan, D. A.; Micevski, D.; Truscott, K. N. The N-End Rule Pathway: From Recognition by N-Recognins, to Destruction by AAA +proteases. *Biochim. Biophys. Acta, Mol. Cell Res.* **2012**, *1823* (1), 83−91.
(33) Varshavsky, A. Discovery of Cellular Regulation by Protein Degradation. *J. Biol. Chem.* **2008**, *283* (50), 34469−34489.
(34) Tasaki, T.; Kwon, Y. T. The Mammalian N-End Rule Pathway: New Insights into Its Components and Physiological Roles. *Trends Biochem. Sci.* **2007**, *32* (11), 520−528.
(35) Mogk, A.; Schmidt, R.; Bukau, B. The N-End Rule Pathway for Regulated Proteolysis: Prokaryotic and Eukaryotic Strategies. *Trends Cell Biol.* **2007**, *17* (4), 165−172.
(36) Varshavsky, A. The N-End Rule Pathway and Regulation by Proteolysis. *Protein Sci. Publ. Protein Soc.* **2011**, *20* (8), 1298−1345.
(37) Sriram, S. M.; Kim, B. Y.; Kwon, Y. T. The N-End Rule Pathway: Emerging Functions and Molecular Principles of Substrate Recognition. *Nat. Rev. Mol. Cell Biol.* **2011**, *12* (11), 735−747.
(38) Luo, J.; Uprety, R.; Naro, Y.; Chou, C.; Nguyen, D. P.; Chin, J. W.; Deiters, A. Genetically Encoded Optochemical Probes for Simultaneous Fluorescence Reporting and Light Activation of Protein Function with Two-Photon Excitation. *J. Am. Chem. Soc.* **2014**, *136* (44), 15551−15558.
(39) Lévy, F.; Johnsson, N.; Rümenapf, T.; Varshavsky, A. Using Ubiquitin to Follow the Metabolic Fate of a Protein. *Proc. Natl. Acad. Sci. U. S. A.* **1996**, *93* (10), 4907−4912.
(40) Suzuki, T. Degradation Signals in the Lysine-Asparagine Sequence Space. *EMBO J.* **1999**, *18* (21), 6017−6026.
(41) Choi, W. S.; Jeong, B.-C.; Joo, Y. J.; Lee, M.-R.; Kim, J.; Eck, M. J.; Song, H. K. Structural Basis for the Recognition of N-End Rule Substrates by the UBR Box of Ubiquitin Ligases. *Nat. Struct. Mol. Biol.* **2010**, *17* (10), 1175−1181.
(42) Liu, Z.; Chen, O.; Wall, J. B. J.; Zheng, M.; Zhou, Y.; Wang, L.; Ruth Vaseghi, H.; Qian, L.; Liu, J. Systematic Comparison of 2A Peptides for Cloning Multi-Genes in a Polycistronic Vector. *Sci. Rep.* **2017**, *7* (1), 2193.
(43) Veeman, M. T.; Slusarski, D. C.; Kaykas, A.; Louie, S. H.; Moon, R. T. Zebrafish Prickle, a Modulator of Noncanonical Wnt/Fz Signaling, Regulates Gastrulation Movements. *Curr. Biol.* **2003**, *13* (8), 680−685.
(44) Schneider-Poetsch, T.; Ju, J.; Eyler, D. E.; Dang, Y.; Bhat, S.; Merrick, W. C.; Green, R.; Shen, B.; Liu, J. O. Inhibition of Eukaryotic Translation Elongation by Cycloheximide and Lactimidomycin. *Nat. Chem. Biol.* **2010**, *6* (3), 209−217.
(45) Mebratu, Y. A.; Negasi, Z. H.; Dutta, S.; Rojas-Quintero, J.; Tesfaigzi, Y. Adaptation of Proteasomes and Lysosomes to Cellular Environments. *Cells* **2020**, *9* (10), 2221.

https://doi.org/10.1021/jacs.1c04324
J. Am. Chem. Soc. 2021, 143, 9222−9229

(46) Bianchi, G.; Oliva, L.; Cascio, P.; Pengo, N.; Fontana, F.; Cerruti, F.; Orsi, A.; Pasqualetto, E.; Mezghrani, A.; Calbi, V.; Palladini, G.; Giuliani, N.; Anderson, K. C.; Sitia, R.; Cenci, S. The Proteasome Load versus Capacity Balance Determines Apoptotic Sensitivity of Multiple Myeloma Cells to Proteasome Inhibition. *Blood* **2009**, *113* (13), 3040−3049.
(47) Kors, S.; Geijtenbeek, K.; Reits, E.; Schipper-Krom, S. Regulation of Proteasome Activity by (Post-)Transcriptional Mechanisms. *Front. Mol. Biosci.* **2019**, *6*, 6.
(48) Zhou, W.; Wesalo, J. S.; Liu, J.; Deiters, A. Genetic Code Expansion in Mammalian Cells: A Plasmid System Comparison. *Bioorg. Med. Chem.* **2020**, *28* (24), 115772.
(49) Shaaya, M.; Fauser, J.; Karginov, A. V. Optogenetics: The Art of Illuminating Complex Signaling Pathways. *Physiology* **2021**, *36* (1), 52−60.
(50) Kwon, E.; Heo, W. D. Optogenetic Tools for Dissecting Complex Intracellular Signaling Pathways. *Biochem. Biophys. Res. Commun.* **2020**, *527* (2), 331−336.
(51) Low, H. B.; Zhang, Y. Regulatory Roles of MAPK Phosphatases in Cancer. *Immune Netw.* **2016**, *16* (2), 85.
(52) Tsang, M.; Maegawa, S.; Kiang, A.; Habas, R.; Weinberg, E.; Dawid, I. B. A Role for MKP3 in Axial Patterning of the Zebrafish Embryo. *Development* **2004**, *131* (12), 2769−2779.
(53) Brunet, A.; Roux, D.; Lenormand, P.; Dowd, S.; Keyse, S.; Pouysségur, J. Nuclear Translocation of P42/P44 Mitogen-activated Protein Kinase Is Required for Growth Factor-induced Gene Expression and Cell Cycle Entry. *EMBO J.* **1999**, *18* (3), 664−674.
(54) Courtney, T. M.; Deiters, A. Optical Control of Protein Phosphatase Function. *Nat. Commun.* **2019**, *10* (1), 4384.
(55) Regot, S.; Hughey, J. J.; Bajar, B. T.; Carrasco, S.; Covert, M. W. High-Sensitivity Measurements of Multiple Kinase Activities in Live Single Cells. *Cell* **2014**, *157* (7), 1724−1734.
(56) Lake, D.; Corrêa, S. A. L.; Müller, J. Negative Feedback Regulation of the ERK1/2 MAPK Pathway. *Cell. Mol. Life Sci.* **2016**, *73* (23), 4397−4413.
(57) Caunt, C. J.; Sale, M. J.; Smith, P. D.; Cook, S. J. MEK1 and MEK2 Inhibitors and Cancer Therapy: The Long and Winding Road. *Nat. Rev. Cancer* **2015**, *15* (10), 577−592.
(58) Lemieux, É.; Bergeron, S.; Durand, V.; Asselin, C.; Saucier, C.; Rivard, N. Constitutively Active MEK1 Is Sufficient to Induce Epithelial-to-Mesenchymal Transition in Intestinal Epithelial Cells and to Promote Tumor Invasion and Metastasis. *Int. J. Cancer* **2009**, *125* (7), 1575−1586.
(59) Costa, M.; Marchi, M.; Cardarelli, F.; Roy, A.; Beltram, F.; Maffei, L.; Ratto, G. M. Dynamic Regulation of ERK2 Nuclear Translocation and Mobility in Living Cells. *J. Cell Sci.* **2006**, *119* (23), 4952−4963.
(60) Brown, W.; Liu, J.; Deiters, A. Genetic Code Expansion in Animals. *ACS Chem. Biol.* **2018**, *13* (9), 2375−2386.

https://doi.org/10.1021/jacs.1c04324
J. Am. Chem. Soc. 2021, 143, 9222−9229